Published for SISSA by Springer

Received: March 28, 2025
Revised: June 3, 2025
Accepted: June 6, 2025
Published: July 4, 2025

Exploring Efimov states in $D^*D^*D^*$ and DD^*D^* three-body systems

Hai-Long Fu,[a,b] **Yong-Hui Lin**,[c] **Feng-Kun Guo**,[a,b,d] **Hans-Werner Hammer**,[c,e] **Ulf-G. Meißner**,[f,g,d] **Akaki Rusetsky**[f,h] **and Xu Zhang**[a]

[a] *CAS Key Laboratory of Theoretical Physics, Institute of Theoretical Physics, Chinese Academy of Sciences, Beijing 100190, China*
[b] *School of Physical Sciences, University of Chinese Academy of Sciences, Beijing 100049, China*
[c] *Institut für Kernphysik, Technische Universität Darmstadt, 64289 Darmstadt, Germany*
[d] *Peng Huanwu Collaborative Center for Research and Education, International Institute for Interdisciplinary and Frontiers, Beihang University, Beijing 100191, China*
[e] *ExtreMe Matter Institute EMMI and Helmholtz Forschungsakademie Hessen für FAIR (HFHF), GSI Helmholtzzentrum für Schwerionenforschung GmbH, 64291 Darmstadt, Germany*
[f] *Helmholtz-Institut für Strahlen- und Kernphysik (Theorie) and Bethe Center for Theoretical Physics, Universität Bonn, D-53115 Bonn, Germany*
[g] *Institute for Advanced Simulation (IAS-4), Forschungszentrum Jülich, D-52425 Jülich, Germany*
[h] *Tbilisi State University, 0186 Tbilisi, Georgia*

E-mail: fuhailong@itp.ac.cn, yonghui.lin@tu-darmstadt.de, fkguo@itp.ac.cn, Hans-Werner.Hammer@physik.tu-darmstadt.de, meissner@hiskp.uni-bonn.de, rusetsky@hiskp.uni-bonn.de, zhangxu@itp.ac.cn

Abstract: The Efimov effect is an intriguing three-body quantum phenomenon. Searching for Efimov states within the realms of nuclear and hadronic physics presents a challenge due to the inherent inability of natural physical systems to exhibit adjustable two-body scattering lengths. In this study, we examine the potential existence of Efimov states in the $D^*D^*D^*$ and DD^*D^* three-hadron systems. Utilizing a pionless effective field theory framework, we determine that the presence of Efimov states in the spectrum of the $D^*D^*D^*$ system is contingent upon the existence of an $(I, J) = (1, 2)$ D^*D^* two-body bound system. If only the T_{cc}^+ and its heavy quark spin partner T_{cc}^{*+} exist while there is no near-threshold pole in all other S-wave $D^{(*)}D^*$ scattering amplitudes, no Efimov effect is expected in the $D^{(*)}D^*D^*$ systems.

Keywords: Effective Field Theories of QCD, Properties of Hadrons

ArXiv ePrint: 2503.19709

https://doi.org/10.1007/JHEP07(2025)081

JHEP07(2025)081

Contents

1 Introduction

Over the past two decades, a large amount of exotic hadronic states has been extensively investigated both experimentally and theoretically. These states demonstrate characteristics that cannot be adequately accounted for by the conventional quark model and investigations may lead to a deeper understanding of nonperturbative quantum chromodynamics (QCD), as discussed in numerous comprehensive reviews [1–16]. The observation of complex structures in proximity to the thresholds of specific hadron pairs suggests that hadronic molecules provide a compelling interpretative framework for these phenomena [6].[1]

The concept of two-body hadronic molecules naturally extends to three-body systems (as recently reviewed in ref. [15]), analogous to multi-nucleon atomic nuclei. The theoretical methodologies for three-body systems, particularly for multi-nucleon systems, have been developed since many years ago, as documented in refs. [22–29]. In recent years, various effective field theory (EFT) frameworks for three-body systems in both finite and infinite volumes have been proposed [30–45]. Furthermore, these methods are applicable for extracting three-body interaction information from lattice QCD data, as demonstrated in refs. [46–56].

The Efimov effect is a remarkable phenomenon in three-body physics [57]. It provides a universal binding mechanism for three-body systems independent of the details of their interactions at short distances. In its simplest setting, it states that in a system of three identical bosons, when the interaction between two particles approaches the unitarity limit (that is when the pair scattering length a is much larger than the range of the interaction R and approaches infinity), a geometric spectrum of infinitely many three-body bound states

[1] This statement holds as long as there are no Castillejo-Dalitz-Dyson (CDD) zeros [17] in the scattering amplitude in the vicinity of the threshold (see, e.g., refs. [18–20]). Until experimental evidence of such additional zeros is obtained, it is most natural to employ the Occam's razor principle to assume the smallest possible number of poles required by data and theory constraints in the scattering amplitude, as discussed in ref. [21].

JHEP07(2025)081

emerges. The ratio of the binding energies (E_n) of these bound states follows the scaling law:

$$\frac{E_n}{E_{n+1}} \approx 515. \tag{1.1}$$

The exact unitary limit ($1/a \to 0, R \to 0$) is a theoretical construct and cannot be reached experimentally (but it is possible to tune $1/a$ to zero in ultracold atoms using Feshbach resonances [58]). However, the predictions of Efimov universality also apply for finite scattering length if $|a| \gg R$ (see ref. [59] for a review). Three-body bound states are usually considered Efimov states if they can be described by Efimov's universal equation with small range corrections [60, 61]. In particular, the ratio of subsequent Efimov states can deviate significantly from the scaling law, eq. (1.1), close to the threshold if $|a| \gg R$ is finite [59]. Experimental evidence for the existence of an Efimov trimer was first found in 2006 in a gas of ultracold Cs atoms [62] by observing a unique three-body loss signature [59] that can be detected by varying the scattering length using the Feshbach resonance technique. Since then, Efimov states have been observed for many bosonic and fermionic atoms as well as atomic mixtures (see ref. [63] for a review of these efforts).

The observation of Efimov physics in nuclear and particle physics systems is hindered by the lack of experimental control over the scattering length [64]. Nevertheless, the triton and certain two-neutron halo nuclei can be considered approximate Efimov states, see, e.g., refs. [65–67]. Moreover, the recent identification of new hadronic states, such as $X(3872)$ and T_{cc}^+, which are situated in the immediate vicinity of relevant two-body thresholds [68, 69] opens up the potential to investigate the possible presence of Efimov states within three-body charmed hadron systems [64, 70–73].

There have already been some results for three-charm systems using different methods [71, 74–79]. In particular, the emergence of the Efimov effect in the $D^*D^*D^*$ system has been explored in ref. [78], under the assumption that a D^*D^* molecule with quantum numbers $(I)J^P = (0)1^+$ exists as the heavy partner of the T_{cc}^+. In this paper, we will examine the existence of the Efimov effect in the $D^*D^*D^*$ and DD^*D^* systems using a systematic nonrelativistic EFT method, which is more convenient for treating all channels with different quantum numbers. We assume the existence of an isoscalar heavy spin partner of the T_{cc}, referred to as T_{cc}^*, which lies close to and below the D^*D^* threshold, as predicted from the existence of $T_{cc}(3875)$ using heavy quark spin symmetry in refs. [80, 81].[2] Both the T_{cc} and T_{cc}^* tetraquark states are characterized by the quantum numbers $(I, J) = (0, 1)$, and they strongly couple to the DD^* and D^*D^* channels in S-wave, respectively. In section 2, we construct the scattering equations for different spin configurations ($T_{cc}D^*$ and $T_{cc}^*D^*$) within a pionless EFT, for all of which the total isospin is $I = 1/2$. Section 3 will address the necessary conditions for the occurrence of the Efimov effect in the full $D^*D^*D^*$ system with all possible (I, J) quantum numbers. A summary is given in the last section.

[2]The hadronic and radiative decays of the T_{cc}^* have been investigated in refs. [82, 83]. The existence of an isoscalar D^*D^* bound state and its width were also investigated in refs. [84, 85].

JHEP07(2025)081

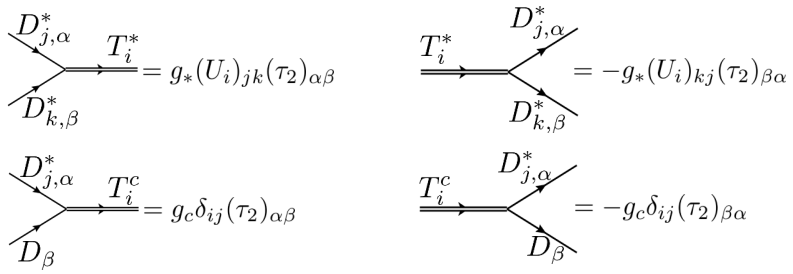

Figure 1. Feynman rules for the dimer-particle couplings from the Lagrangian in eq. (2.1).

2 $D^*D^*D^*$ and DD^*D^* in NREFT

2.1 Effective Lagrangian and propagators

In an energy range very close to the threshold, the system can be described by a pionless EFT, which is dominated by contact interaction terms, as discussed in, e.g., refs. [70, 86–88]. We consider that there is an isoscalar T_{cc} near-threshold bound state in the S-wave DD^* channel [69, 89] and an isoscalar T^*_{cc} near-threshold bound state in the S-wave D^*D^* channel as predicted in refs. [80, 81], and in this section we assume that there are no other near-threshold S-wave poles in two-body double-charm systems.[3]

The effective Lagrangian including the T_{cc} and T^*_{cc} dimer fields is given by

$$\begin{aligned}\mathcal{L} =& D^{*\dagger}_{i\alpha}\left(i\partial_0 + \frac{\nabla^2}{2M_D}\right)D^*_{i\alpha} + D^\dagger_\alpha\left(i\partial_0 + \frac{\nabla^2}{2M_{D^*}}\right)D_\alpha + T^{*\dagger}_i\Delta_* T^*_i + T^{c\dagger}_i\Delta_c T^c_i \\ &- g_*\left[T^{*\dagger}_i D^*_{j\alpha}(U_i)_{jk}(i\tau_2)_{\alpha\beta}D^*_{k\beta} + \text{h.c.}\right] - g_c\left[T^{c\dagger}_i D^*_{j\alpha}\delta_{ij}(i\tau_2)_{\alpha\beta}D_\beta + \text{h.c.}\right],\end{aligned} \tag{2.1}$$

where D and D^* denote the pseudoscalar and vector charm meson fields, respectively, while T^* and T^c represent the dimer fields that annihilate the T^*_{cc} and T_{cc} states, respectively. The lower-case Latin letters $i, j, k \in \{1, 2, 3\}$ serve as spin-1 indices, and the Greek lower-case letters $\alpha, \beta \in \{1, 2\}$ represent isospin-1/2 indices. The second Pauli matrix τ_2 operates in the isospin space, while the U_i's are the generators of the rotation group acting on the spin-1 representation, with matrix elements $(U_i)_{jk} = -i\epsilon_{ijk}$. The parameters g_* and g_c characterize the coupling strengths between the dimer fields and their constituent particles. At leading order, $g_{*,c}$ and $\Delta_{*,c}$ are not independent parameters, and only the combinations $g^2_{*,c}/\Delta_{*,c}$ appear in physical observables. The dimer-particle couplings are depicted in figure 1.

The two-body scattering amplitude is proportional to the propagator of the dimer field. The dressed propagator G_A is given by:

$$iG_A(p_0, \mathbf{p})_{ij} = \frac{i\delta_{ij}}{\Delta_A + c_A\Sigma_A(p_0, \mathbf{p})}, \tag{2.2}$$

where $A = *, c$ is the dimer index, and Σ_A is the self-energy function. The spin and isospin operators between the dimer and meson fields contribute a Kronecker delta δ_{ij} in

[3] It was found in recent lattice QCD calculations that both the isovector S-wave DD^* [90] and DD [91] systems are repulsive.

JHEP07(2025)081

the numerator and a normalization constant c_A in the denominator. For the propagator G_*, $c_* = 4$, while for G_c, $c_c = 2$.

The ultraviolet (UV) divergence in the self-energy can be regularized using the power divergence subtraction scheme with a hard scale $\Lambda_{\rm PDS}$ [92, 93] as

$$\Sigma_A(p_0, \mathbf{p}) = \frac{1}{2\pi} g_A^2 S_{2,A} \mu_A \left[-\sqrt{-2\mu_A \left(p_0 - \frac{p^2}{2M_A} \right) - i\varepsilon} + \Lambda_{\rm PDS} \right], \tag{2.3}$$

where $S_{2,A}$ represents the symmetry factor associated with the exchange of identical particles in Σ_A (for the D^*D^* and DD^* dimers, $S_{2,*} = 2$ and $S_{2,c} = 1$, respectively), and p_0 and $\mathbf{p}$ are the energy and three-momentum of the dimer, with p denoting the magnitude of $\mathbf{p}$. Here, μ_A and M_A denote the reduced mass and total mass of the constituent particles, respectively. Specifically, $\mu_c = M_D M_{D^*}/M_c$ with $M_c = M_D + M_{D^*}$ for the DD^* system, and $\mu_* = M_{D^*} M_{D^*}/M_*$ with $M_* = 2M_{D^*}$ for the D^*D^* system.

The renormalized propagators for the T_{cc}^* and T_{cc} dimers are then obtained as follows:

$$\begin{aligned} iG_*(p_0, \mathbf{p})_{ij} &= iG_*(p_0, \mathbf{p})\delta_{ij} = -\frac{2\pi i}{g_*^2 \mu_* S_{2,*} c_*} \frac{\delta_{ij}}{-1/a_* + \sqrt{-2\mu_*(p_0 - \frac{\mathbf{p}^2}{2M_*} + i\varepsilon)}}, \\ iG_c(p_0, \mathbf{p})_{ij} &= iG_c(p_0, \mathbf{p})\delta_{ij} = -\frac{2\pi i}{g_c^2 \mu_c S_{2,c} c_c} \frac{\delta_{ij}}{-1/a_c + \sqrt{-2\mu_c(p_0 - \frac{\mathbf{p}^2}{2M_c} + i\varepsilon)}}, \end{aligned} \tag{2.4}$$

The UV divergence in the self-energy has been absorbed into the scattering length through the relation

$$\frac{1}{a_A} = \frac{2\pi \Delta_A}{g_A^2 \mu_A S_{2,A} c_A} + \Lambda_{\rm PDS}. \tag{2.5}$$

The value of a_A determines the pole position of the two-body subsystem, with a positive a corresponding to a bound state and a negative a corresponding to a virtual state.[4] Furthermore, the wave function renormalization constants Z_* and Z_c, which are obtained from the residue at the pole are given by

$$Z_* = \frac{2\pi\gamma_*}{g_*^2 \mu_*^2 S_{2,*} c_*}, \quad Z_c = \frac{2\pi\gamma_c}{g_c^2 \mu_c^2 S_{2,c} c_c}, \tag{2.6}$$

where $\gamma_A = \pm\sqrt{2\mu_A |E_B^A|}$ ($A = *, c$ for T_{cc}^* and T_{cc}, respectively) denotes the binding momentum with the positive (negative) sign for a bound (virtual) state pole and E_B^A the corresponding binding energy.

2.2 Three-body scattering equations

Using the particle-dimer Lagrangian, we can derive the scattering equation for the three-body system. Our calculations are performed in the center-of-mass (c.m.) frame of the

[4] For a repulsive potential, the scattering length has the same sign as that in the case with one bound state, but the magnitude is much smaller such that the pole is very far below 2-body threshold and thus beyond the applicable range of theory.

JHEP07(2025)081

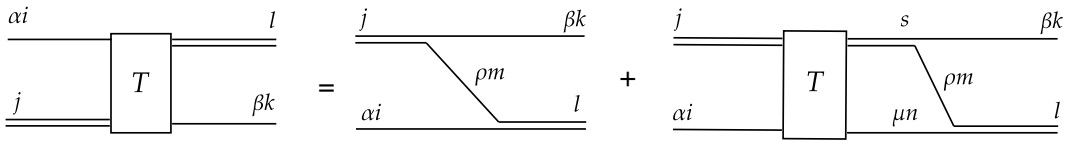

Figure 2. Integral equation for the $T_{cc}^* D^*$ scattering amplitude T with incoming isospin index α and spin indices i, j, and outgoing indices β and k, l. Here, the single solid line represents the D^* meson while the double solid line denotes the $D^* D^*$ dimer T_{cc}^*.

corresponding spectator-dimer system, such as the $D^{(*)} T_A$ system. The total energy E is expressed as:

$$E = \frac{q^2}{2M_A} + \frac{q^2}{2M_{\rm sp}} - \frac{\gamma_A^2}{2\mu_A}, \tag{2.7}$$

where $M_{\rm sp} = M_D(M_{D^*})$ is the mass of the spectator, $M_A = M_*(M_c)$ is the total mass of the two particles in the two-body subsystem, and q is the momentum of the spectator.

We analyze the scattering equation to investigate possible bound states. The absence of the strong cutoff dependence of observables (e.g., the scattering amplitudes) in our calculations indicates that there are no bound states in the corresponding channel [71, 88, 94]. Conversely, the emergence of three-body bound states signals the Efimov effect. In such cases, the integral equation, which includes only two-body interactions, exhibits significant cutoff dependence, necessitating the inclusion of three-body contact interactions for renormalization [86, 94]. For the scattering equation of three identical particles in various partial wave channels, the existence of the Efimov effect depends on the coefficients in the scattering equation of the system under investigation [59, 87]. These coefficients include contributions from the Clebsch-Gordan (CG) coefficients of (iso)spin coupling and the symmetry factor of identical particles. A systematic analysis, for which the dimers are not restricted to the T_{cc}^* and T_{cc}, will be presented in the subsequent section.

2.3 $T_{cc}^* D^*$ Scattering

We begin with the single-channel $T_{cc}^* D^*$ scattering, whose amplitude T satisfies the integral equation shown in figure 2. Before proceeding further, let us present the independent tree-level amplitudes for the $T^{*(c)} D^{(*)}$ systems. Using the vertex factors shown in figure 1, we have

$$\begin{aligned}
i\mathcal{M}^{ji\alpha\to lk\beta}_{T^*D^*\to T^*D^*}(E,\mathbf{k},\mathbf{p}) &= \frac{-ig_*^2 S_{3,1}(U_l U_j)_{ik}\delta_{\beta\alpha}}{E - \frac{k^2}{2M_{D^*}} - \frac{p^2}{2M_{D^*}} - \frac{(\mathbf{k}+\mathbf{p})^2}{2M_{D^*}} + i\varepsilon}, \\
i\mathcal{M}^{i\alpha\to jk\beta}_{T^*D\to T_cD^*}(E,\mathbf{k},\mathbf{p}) &= \frac{-ig_* g_c S_{3,2}(U_i)_{kj}\delta_{\beta\alpha}}{E - \frac{k^2}{2M_{D}} - \frac{p^2}{2M_{D^*}} - \frac{(\mathbf{k}+\mathbf{p})^2}{2M_{D^*}} + i\varepsilon}, \\
i\mathcal{M}^{ji\alpha\to lk\beta}_{T_cD^*\to T_cD^*}(E,\mathbf{k},\mathbf{p}) &= \frac{-ig_c^2 S_{3,3}\delta_{il}\delta_{kj}\delta_{\beta\alpha}}{E - \frac{k^2}{2M_{D^*}} - \frac{p^2}{2M_{D^*}} - \frac{(\mathbf{k}+\mathbf{p})^2}{2M_{D}} + i\varepsilon}, \\
i\mathcal{M}^{ji\alpha\to k\beta}_{T_cD^*\to T^*D}(E,\mathbf{k},\mathbf{p}) &= \frac{-ig_* g_c S_{3,4}(U_k)_{ji}\delta_{\beta\alpha}}{E - \frac{k^2}{2M_{D^*}} - \frac{p^2}{2M_{D}} - \frac{(\mathbf{k}+\mathbf{p})^2}{2M_{D^*}} + i\varepsilon},
\end{aligned} \tag{2.8}$$

JHEP07(2025)081

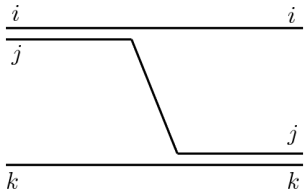

Figure 3. Diagram for particle-dimer scattering via the particle exchange. Here i, j and k refer to particles.

where $\mathbf{k}, \mathbf{p}$ represent the outgoing and incoming 3-momenta, respectively. $S_{3,i}$ is the symmetry factor for each one-boson-exchange diagram, with $S_{3,1} = 4$, $S_{3,2} = S_{3,4} = 2$ and $S_{3,3} = 1$. These symmetry factors due to the exchange of identical particles are given by (see figure 3)

$$S_{ijk} = \begin{cases} 4 \text{ if } i = j = k, \\ 2 \text{ if } i \neq j = k \text{ or } i = j \neq k, \\ 1 \text{ if } i = k \neq j. \end{cases} \tag{2.9}$$

The integral equation for the $T_{cc}^* D^*$ scattering is given by

$$\begin{aligned} t_{ji\alpha}^{lk\beta}(E, \mathbf{k}, \mathbf{p}) &= \mathcal{M}_{T^*D^* \to T^*D^*}^{ji\alpha \to lk\beta}(E, \mathbf{k}, \mathbf{p}) \\ &+ \int \frac{d^4q}{(2\pi)^4} \frac{i\mathcal{M}_{T^*D^* \to T^*D^*}^{sn\mu \to lk\beta}(E, \mathbf{q}, \mathbf{p})}{-q_0 - \frac{q^2}{2M_{D^*}} + i\varepsilon} \times \frac{2\pi}{g_*^2 \mu_*} \frac{1}{S_{2,*} c_*} \frac{t_{ji\alpha}^{sn\mu}(E, \mathbf{k}, \mathbf{q})}{-\gamma_* + \sqrt{-2\mu_* \left(E + q_0 - \frac{q^2}{2M_*}\right) - i\varepsilon}}, \end{aligned} \tag{2.10}$$

where $t_{ji\alpha}^{lk\beta}$ is the scattering amplitude that includes the complete spin-isospin structure. After integrating over the q_0 component and multiplying by the wave function renormalization constant, we obtain

$$\begin{aligned} T_{ji\alpha}^{lk\beta}(E, \mathbf{k}, \mathbf{p}) &= -\frac{\pi \gamma_*}{\mu_*^2} \frac{2S_{3,1}}{S_{2,*} c_*} \frac{(U_l U_j)_{ik} \delta_{\beta\alpha}}{E - \frac{k^2}{2M_{D^*}} - \frac{p^2}{2M_{D^*}} - \frac{(\mathbf{k}+\mathbf{p})^2}{2M_{D^*}} + i\varepsilon} \\ &- \frac{\pi}{\mu_*} \frac{2S_{3,1}}{S_{2,*} c_*} \int \frac{d^3q}{(2\pi)^3} \frac{T_{ji\alpha}^{sn\mu}(E, \mathbf{k}, \mathbf{q})}{-\gamma_* + \sqrt{-2\mu_* \left(E - \frac{q^2}{2M_{D^*}} - \frac{q^2}{2M_*}\right) - i\varepsilon}} \frac{(U_l U_s)_{nk} \delta_{\beta\mu}}{E - \frac{q^2}{2M_{D^*}} - \frac{p^2}{2M_{D^*}} - \frac{(\mathbf{q}+\mathbf{p})^2}{2M_{D^*}} + i\varepsilon}, \end{aligned} \tag{2.11}$$

with $T_{ji\alpha}^{lk\beta} \equiv Z_* \, t_{ji\alpha}^{lk\beta}$.

$T_{ji\alpha}^{lk\beta}$ can be projected onto a general partial wave,

$$\frac{1}{2} \int_{-1}^{+1} d\cos\theta \, P_L(\cos\theta) \, T(E, \mathbf{k}, \mathbf{p}) = T_{(L)}(E, k, p) \, , \tag{2.12}$$

where θ is the angle between $\mathbf{k}$ and $\mathbf{p}$, $P_L(\cos\theta)$ is the Legendre polynomial of order L. For

$L=0$, we obtain the integral equation for the S-wave $T_{cc}^*D^*$ scattering amplitude

$$\begin{aligned}
T_{(0)\,ji\alpha}^{\;\;lk\beta}(E,k,p) =& -\frac{\pi\gamma_*}{\mu_*^2}\frac{2S_{3,1}}{S_{2,*}c_*}V_1^S(k,p)\boxed{(U_lU_j)_{ik}\,\delta_{\beta\alpha}} \\
&-\frac{1}{\pi\mu_*}\frac{S_{3,1}}{S_{2,*}c_*}\int_0^\Lambda dq\frac{q^2\,V_1^S(q,p)\,T_{(0)\,ji\alpha}^{\;\;sn\mu}(E,k,q)\boxed{(U_lU_s)_{nk}\,\delta_{\beta\mu}}}{-\gamma_*+\sqrt{-2\mu_*\left(E-\frac{q^2}{2M_{D^*}}-\frac{q^2}{2M_*}\right)-i\varepsilon}} \\
\equiv& \mathcal{M}_0\boxed{C_{0\;ji\alpha}^{\;\;lk\beta}}+\int_0^\Lambda dq\,\mathcal{M}_1 T_{(0)\,ji\alpha}^{\;\;sn\mu}(E,k,q)\boxed{C_{0\;sn\mu}^{\;\;lk\beta}},
\end{aligned} \tag{2.13}$$

where Λ is the UV cutoff discussed above. The last equality defines the amplitudes $\mathcal{M}_0$, $\mathcal{M}_1$ and the coefficients $C_{0\;ji\alpha}^{\;\;lk\beta}$ and $C_{0\;sn\mu}^{\;\;lk\beta}$; for the latter we use boxed notations to make the corresponding definitions more transparent (similar notations will be used later). The S-wave potential V^S is given by

$$V_1^S(k,q) = -\frac{M_{D^*}}{kp}Q_0\left(-\frac{M_{D^*}}{kp}\left(E-\frac{k^2}{2\mu_*}-\frac{p^2}{2\mu_*}\right)-i\varepsilon\right). \tag{2.14}$$

The logarithmic function Q_0 originates from the one-meson exchange contributions, whose S-wave projection leads to integrals of the form

$$Q_0(\beta) \equiv \frac{1}{2}\int_{-1}^{+1}dx\frac{P_0(x)}{x+\beta} = \frac{1}{2}\ln\left(\frac{\beta+1}{\beta-1}\right). \tag{2.15}$$

For the S-wave $T_{cc}^*D^*$ system, all possible quantum numbers are $J^P=0^-,1^-$ and 2^-. Following ref. [87], we project out the desired channel with a given isospin I and angular momentum J by evaluating:

$$T_{(0)}^{I,J} \equiv \frac{1}{(2J+1)(2I+1)}\sum_{\tilde{m}\tilde{\eta},\tilde{n}\tilde{\lambda}}\mathcal{O}^\dagger_{\tilde{n}\tilde{\lambda},\tilde{j}\tilde{\beta}}\,T_{(0)\,\tilde{i}\tilde{\alpha}}^{\;\;\tilde{j}\tilde{\beta}}\,\mathcal{O}_{\tilde{m}\tilde{\eta},\tilde{i}\tilde{\alpha}}\,, \tag{2.16}$$

where we use the tilded indices to represent both spin and isospin (if any) indices of the given operators. $\tilde{i}\tilde{\alpha}$ and $\tilde{j}\tilde{\beta}$ are the indices for initial and final state spectator-dimer pairs. To be more specific, $\tilde{i}$ ($\tilde{j}$) includes both the spin and isospin indices for the initial (final) D^*, while $\tilde{\alpha}$, $\tilde{\beta}$ are the spin indices for the isoscalar T_{cc}^*. $\tilde{n}\tilde{\lambda}$ and $\tilde{m}\tilde{\eta}$ represent the indices in the corresponding (I,J) channel after projection. It should be noted that for elastic scattering, the initial and final states are identical, requiring $\tilde{\eta}=\tilde{\lambda}$ and $\tilde{m}=\tilde{n}$. The projection operators for the scalar, vector and tensor amplitudes are

$$\begin{aligned}
\mathcal{O}_{ji}^{J=0}(1\otimes 1\to 0) &= \frac{-1}{\sqrt{3}}\delta_{ij}\,, \\
\mathcal{O}_{\ell,mn}^{J=1}(1\otimes 1\to 1) &= \frac{-1}{\sqrt{2}}(U_\ell)_{mn}\,, \\
\mathcal{O}_{\ell k,mn}^{J=2}(1\otimes 1\to 2) &= \frac{1}{2}[\delta_{\ell m}\delta_{kn}+\delta_{\ell n}\delta_{km}-\frac{2}{3}\delta_{\ell k}\delta_{mn}]\,,
\end{aligned} \tag{2.17}$$

and the corresponding isospin projection operator is given by

$$\mathcal{O}_{\alpha,\beta}^{I=1/2}\left(\frac{1}{2}\otimes 0\to\frac{1}{2}\right) = \delta_{\alpha\beta}. \tag{2.18}$$

JHEP07(2025)081

Channel	$(I,J)=(1/2,0)$	$(I,J)=(1/2,1)$	$(I,J)=(1/2,2)$
$C_0^I C_0^J$	$1\times(-2)$	1×1	1×1

Table 1. Coefficients of the partial-wave projected integral equation for the S-wave $T_{cc}^* D^*$ scattering.

Applying the above projections to the integral equation of the S-wave $T_{cc}^* D^*$ scattering, eq. (2.13), one gets

$$\begin{aligned}
T_{(0)}^{I=\frac{1}{2},J=0} \equiv & \frac{1}{2}\sum_{\eta\lambda}\left(\mathcal{O}^{I=1/2}_{\lambda,\beta}\mathcal{O}^{J=0}_{lk}\right)^{\dagger} T_{(0)\,ji\alpha}^{\;\;\;lk\beta}\left(\mathcal{O}^{I=1/2}_{\eta,\alpha}\mathcal{O}^{J=0}_{ji}\right) \\
= & \frac{1}{2}\frac{1}{3}[\delta_{kl}(U_l U_j)_{ik}\delta_{ji}]\left[\sum_{\eta\lambda}\delta_{\beta\lambda}\delta_{\beta\alpha}\delta_{\eta\alpha}\right]\mathcal{M}_0 \\
& + \frac{1}{2}\int_0^\Lambda dq\mathcal{M}_1\sum_{\eta\lambda}\left(\frac{-1}{\sqrt{3}}\delta_{lk}\delta_{\beta\lambda}\right)C_{0\,sn\mu}^{\;\;\;lk\beta}T_{(0)\,ji\alpha}^{\;\;\;sn\mu}\left(\mathcal{O}^{I=1/2}_{\eta,\alpha}\mathcal{O}^{J=0}_{ji}\right) \\
= & \frac{1}{2}\frac{1}{3}\times(-6)\times 2\mathcal{M}_0 + \int_0^\Lambda dq\mathcal{M}_1(-2)\times\frac{1}{2}\sum_{\eta\lambda}\left(\mathcal{O}^{I=1/2}_{\lambda,\mu}\mathcal{O}^{J=0}_{sn}\right)^{\dagger} T_{(0)\,ji\alpha}^{\;\;\;sn\mu}\left(\mathcal{O}^{I=1/2}_{\eta,\alpha}\mathcal{O}^{J=0}_{ji}\right) \\
= & -2\mathcal{M}_0 - 2\int_0^\Lambda dq\mathcal{M}_1 T_{(0)}^{I=\frac{1}{2},J=0},
\end{aligned} \tag{2.19}$$

with two scalar amplitudes $\mathcal{M}_0$ and $\mathcal{M}_1$, which have been defined by the last equality in eq. (2.13). Similarly, applying the spin-isospin projections for other partial waves to eq. (2.13) yields the corresponding integral equations for each partial wave amplitude, all of which can be written in the following general form,

$$T_{(0)}^{I,J}(E,k,p) = C_0^I C_0^J\,\mathcal{M}_0(k,p) + \int_0^\Lambda dq\, C_0^I C_0^J \mathcal{M}_1(p,q) T_{(0)}^{I,J}(E,k,q). \tag{2.20}$$

The spin-isospin coefficients are given in table 1.

The dimer-particle amplitude $T_{(0)}^{I,J}(E,k,p)$, obtained from the integral equations above, contains all physical information relevant to the three-meson system with specified quantum numbers. These include, for instance, the phase shifts of $T^{(*)}$-$D^{(*)}$ scattering and the possible existence of three-body bound states. After discretizing the integral in eq. (2.20), the integral equation can be rewritten as an eigenvalue problem expressed as follows:

$$(1 - C_0^I C_0^J \tilde{\mathcal{M}}_1)\tilde{T}_{(0)}^{I,J} = C_0^I C_0^J \tilde{\mathcal{M}}_0, \tag{2.21}$$

where $\tilde{}$ denotes the discretized form (vector or matrix) of the quantity evaluated on the chosen integral mesh. To explore the existence of such bound states, one can directly identify the poles of the amplitude, which are given as solutions of the following equation:

$$\det(1 - \tilde{V}\tilde{G}) \equiv \det(1 - C_0^I C_0^J \tilde{\mathcal{M}}_1) = 0, \tag{2.22}$$

which is exactly analogous to the strategy used in searching for poles of the two-body scattering amplitude solved from the Lippmann-Schwinger equation.

JHEP07(2025)081

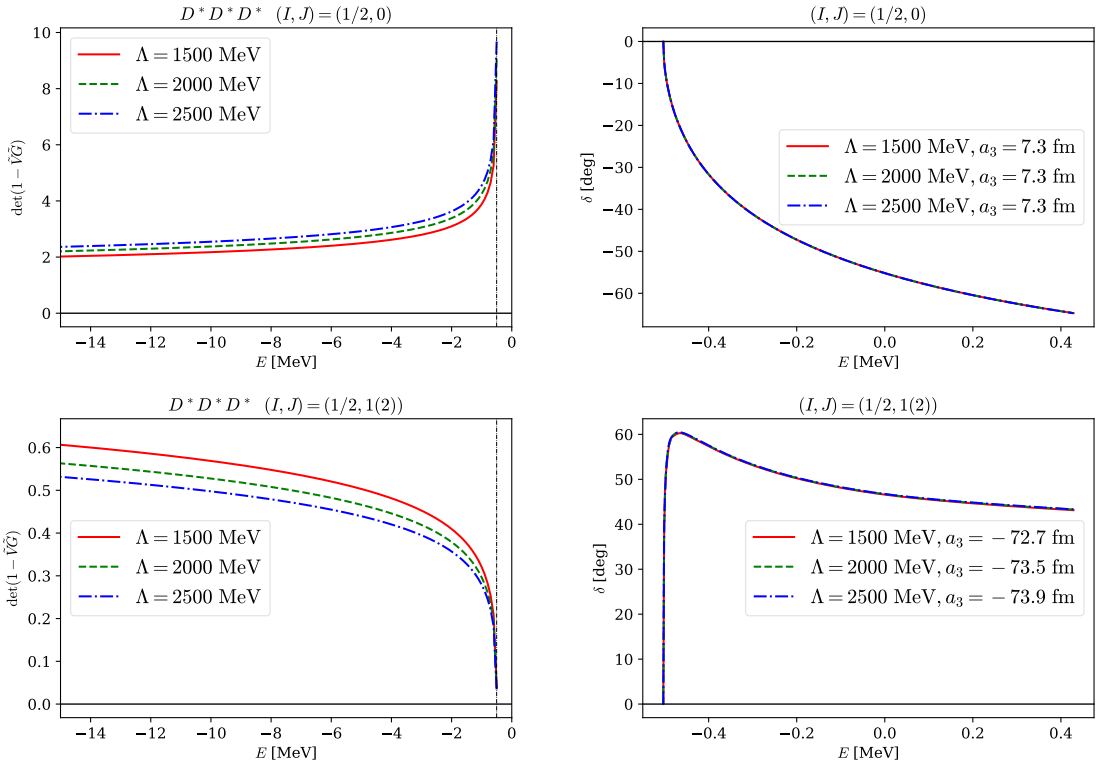

Figure 4. Left panel: determinant $\det(1-\tilde{V}\tilde{G})$ of the $T_{cc}^*D^*$ scattering equation for the channel with quantum numbers $(I,J)=(1/2,0)$ and $(I,J)=(1/2,1(2))$. Right panel: the corresponding S-wave $T_{cc}^*D^*$ scattering phase shifts, for which curves with different cutoffs are almost indistinguishable. The vertical lines denote the $D^*T_{cc}^*$ two-body threshold.

Our results demonstrate that all partial waves exhibit weak cutoff dependence, as shown in the left panel of figure 4. Note that the only theoretical inputs are the binding energies of the two $(I,J)=(0,1)$ dimers, corresponding to physical T_{cc}^* and T_{cc} states, given by $E_B^*=-0.50\,\text{MeV}$ and $E_B^c=-0.36\,\text{MeV}$ [81], respectively. The absence of trimer poles is evident across a wide range of Λ values from 1.5 to 2.5 GeV.[5]

In the right panel of figure 4, we have plotted the corresponding scattering phase shifts of $D^*T_{cc}^*$. One sees that the phase shifts remain almost unchanged when altering the cutoff Λ. In the plot, the $D^*T_{cc}^*$ S-wave scattering length a_3 is also labeled, whose definition is as follows:

$$a_3^{(I,J)} \equiv -\frac{\mu_3}{2\pi} T_{(0)}^{I,J}(k=p=0), \tag{2.23}$$

where $\mu_3 = M_{T_{cc}^*}M_{D^*}/(M_{T_{cc}^*}+M_{D^*})$ is the reduced mass of $D^*T_{cc}^*$. The S-wave phase shifts

[5] A different conclusion was reached in ref. [78] due to inconsistent prefactors arising from the partial wave projection compared to our work. There the existence of a three-body bound state with quantum numbers $(I,J)=(1/2,0)$ in the $D^*D^*D^*$ system was claimed, using a coefficient equivalent to $C_0^{J=0}=4$ in our notation. However, in our case, $C_0^{J=0}=-2$. In fact, as this coefficient changes from 4 to -2, the three-body system undergoes a Berezinskii-Kosterlitz-Thouless-like phase transition [95], leading to the disappearance of the bound state.

JHEP07(2025)081

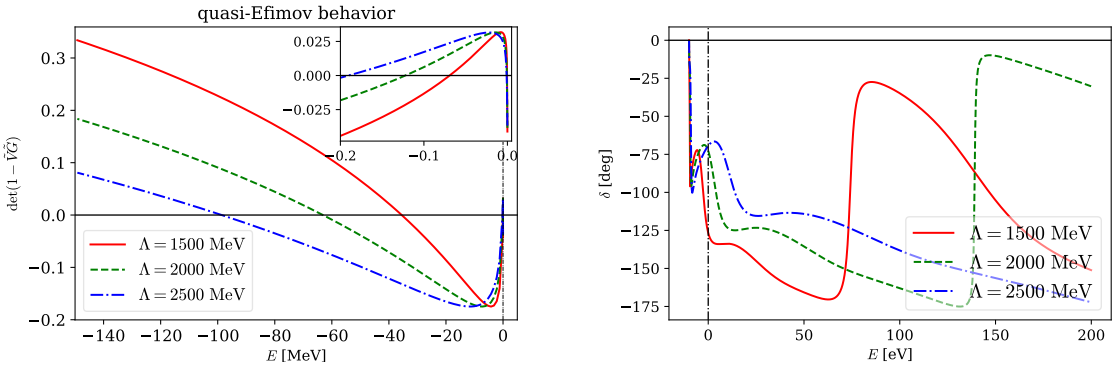

Figure 5. Left panel: determinant $\det(1-\tilde{V}\tilde{G})$ of the scattering equation for three identical scalar bosons with mass $m = M_{D^*}$, illustrating the Efimov behavior. The two-body binding energy is set to 10 eV, and zero-crossings of the determinant indicate three-body bound states. The vertical line denotes the three-body threshold which almost equals to particle-dimer threshold in this binding energy. The inset magnifies the region very near threshold. Right panel: the particle-dimer scattering phase shift. Different from the results in figure 4, the phase shift is very sensitive to Λ.

for $D^*T_{cc}^*$ system are calculated as

$$\delta^{(I,J)} = \text{arccot}\left(\frac{2\pi}{\mu_3}\frac{1}{k}\,\text{Re}\frac{1}{T_{(0)}^{(I,J)}(E,k,k)}\right). \tag{2.24}$$

To illustrate how $\det(1-\tilde{V}\tilde{G})$ and the phase shift would behave if an Efimov state exists (the scattering equation for such a system can be found in refs. [86, 94]), in figure 5 we present a characteristic Efimov scenario with three identical scalar bosons of mass M_{D^*} and a two-body binding energy of 10 eV, the value of which is only for illustration. Notice that no three-body contact term has been included to absorb the cutoff dependence (or in other words, the three-body contact term is set to zero). From the left panel of figure 5, one sees that tuning the two-body binding energy to 10 eV reveals the existence of at least three three-body bound states. The right panel shows that the particle-dimer S-wave phase shift changes drastically within a small energy range due to the presence of multiple near-threshold bound state poles. One also notices that the phase shift is very sensitive to the cutoff, in contrast to the case without any Efimov state in figure 4. The cutoff dependence in both the phase shift and the three-body bound state position can be removed once a three-body contact term is included.

2.4 T_{cc}^*D-$T_{cc}D^*$ coupled-channel scattering

Next, we consider the S-wave T_{cc}^*D-$T_{cc}D^*$ scattering. For total spin $J = 1$, we must solve coupled-channel integral equations since transitions between T_{cc}^*D and $T_{cc}D^*$ are allowed, as illustrated in figure 6. In contrast, for $J = 0$ and $J = 2$, only the single-channel $T_{cc}D^*$ scattering occurs.

The coupled-channel integral equations for the $T_{cc}^*D \to T_{cc}^*D$ scattering amplitude T_1

JHEP07(2025)081

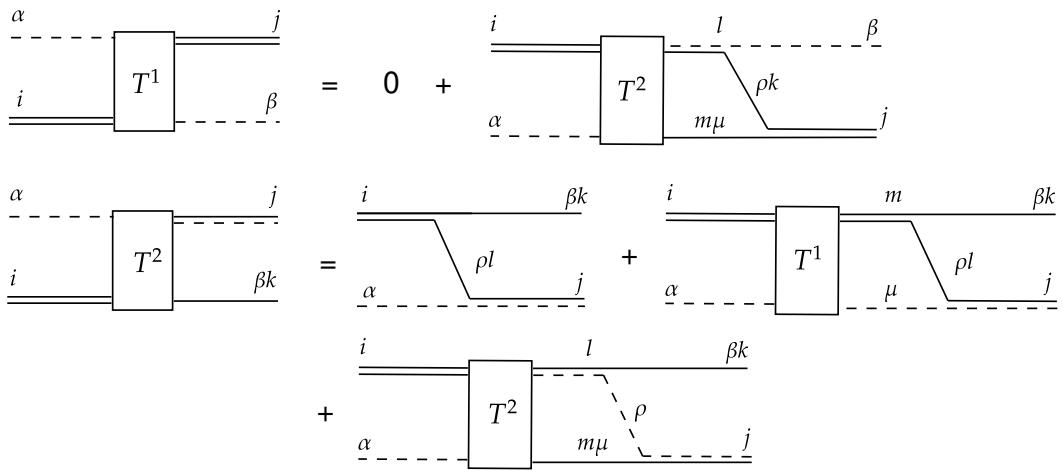

Figure 6. Integral equations for the coupled-channel ($T_{cc}^* D$ and $T_{cc} D^*$) scattering amplitudes. Here, the single solid (dashed) line represents D^* (D) meson, and the double solid (solid-dashed) line represents the $D^* D^*$ ($D D^*$) dimer T_{cc}^* (T_{cc}).

and the $T_{cc}^* D \to T_{cc} D^*$ scattering amplitude T_2 are

$$
\begin{aligned}
(T_1)_{(0)\,i\alpha}^{\;j\beta}(E,k,p) &= -\frac{1}{\pi\mu_*}\frac{S_{3,4}}{S_{2,c}c_c}\int_0^\Lambda dq \sqrt{\frac{\gamma_* S_{2,c} c_c}{\gamma_c S_{2,*} c_*}}\frac{q^2\, V_4^S(q,p)(T_2)_{(0)\,i\alpha}^{\;lm\mu}(E,k,q)\,\boxed{(U_j)_{lm}\delta_{\beta\mu}}}{-\gamma_c+\sqrt{-2\mu_c\left(E-\frac{q^2}{2M_{D^*}}-\frac{q^2}{2M_c}\right)-i\varepsilon}} \\
&\equiv +\int_0^\Lambda dq\, \mathcal{M}_{12}(T_2)_{(0)\,i\alpha}^{\;lm\mu}(E,k,q)\,\boxed{C_{1\,lm\mu}^{\;j\beta}}\,,
\end{aligned}
\tag{2.25}
$$

and

$$
\begin{aligned}
(T_2)_{(0)\,i\alpha}^{\;jk\beta}(E,k,p) =& -\frac{\pi\sqrt{\gamma_*\gamma_c}}{\mu_*\mu_c}\frac{2S_{3,2}}{\sqrt{S_{2,*}c_* S_{2,c}c_c}}V_2^S(k,p)\,\boxed{(U_i)_{kj}\delta_{\beta\alpha}} \\
&-\frac{1}{\pi\mu_c}\frac{S_{3,2}}{S_{2,*}c_*}\int_0^\Lambda dq\sqrt{\frac{\gamma_c S_{2,*}c_*}{\gamma_* S_{2,c}c_c}}\frac{q^2\, V_2^S(q,p)(T_1)_{(0)\,i\alpha}^{\;m\mu}(E,k,q)\,\boxed{(U_m)_{kj}\delta_{\beta\mu}}}{-\gamma_*+\sqrt{-2\mu_*\left(E-\frac{q^2}{2M_D}-\frac{q^2}{2M_*}\right)-i\varepsilon}} \\
&-\frac{1}{\pi\mu_c}\frac{S_{3,3}}{S_{2,c}c_c}\int_0^\Lambda dq\frac{q^2\, V_3^S(q,p)\,(T_2)_{(0)\,i\alpha}^{\;lm\mu}(E,k,q)\,\boxed{\delta_{kl}\delta_{mj}\delta_{\beta\mu}}}{-\gamma_c+\sqrt{-2\mu_c\left(E-\frac{q^2}{2M_{D^*}}-\frac{q^2}{2M_c}\right)-i\varepsilon}} \\
\equiv& \mathcal{M}_{20}\,\boxed{C_{2\,i\alpha}^{\;jk\beta}}+\int_0^\Lambda dq\,\mathcal{M}_{21}(T_1)_{(0)\,i\alpha}^{\;m\mu}(E,k,q)\,\boxed{C_{2\,m\mu}^{\;jk\beta}} \\
&+\int_0^\Lambda dq\,\mathcal{M}_{22}(T_2)_{(0)\,i\alpha}^{\;lm\mu}(E,k,q)\,\boxed{C_{3\,lm\mu}^{\;jk\beta}}\,,
\end{aligned}
\tag{2.26}
$$

where the S-wave projection and wave function renormalization factors have been applied,

Channel	$C_1^I C_1^J$	$C_2^I C_2^J$	$C_3^I C_3^J$
$(I,J)=(\frac{1}{2},1)$	$1\times\sqrt{2}$	$1\times\sqrt{2}$	$1\times(-1)$

Table 2. Coefficients of the partial-wave projected integral equation for the S-wave $T_{cc}^* D$ scattering.

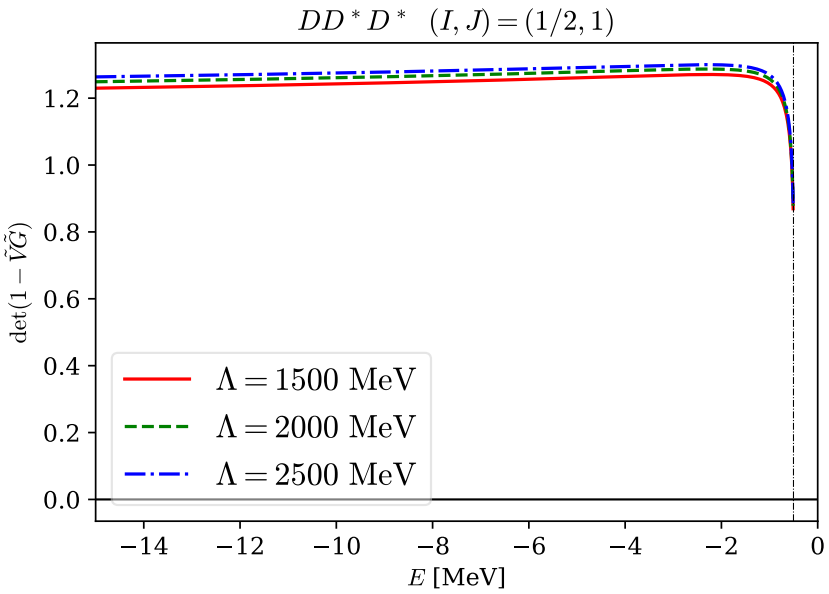

Figure 7. Determinant $\det(1-\tilde{V}\tilde{G})$ of the $T_{cc}^* D$-$T_{cc} D^*$ coupled-channel scattering equations with quantum numbers $(I,J)=(1/2,1)$. The vertical line denotes the threshold of $T_{cc}^* D$.

and the relevant S-wave potentials V^S are given by

$$
\begin{aligned}
V_2^S(k,q) &= -\frac{M_{D^*}}{kp} Q_0\left(-\frac{M_{D^*}}{kp}\left(E-\frac{k^2}{2\mu}-\frac{p^2}{2\mu_*}\right)-i\varepsilon\right) , \\
V_3^S(k,q) &= -\frac{M_D}{kp} Q_0\left(-\frac{M_D}{kp}\left(E-\frac{k^2}{2\mu}-\frac{p^2}{2\mu}\right)-i\varepsilon\right) , \\
V_4^S(k,q) &= -\frac{M_{D^*}}{kp} Q_0\left(-\frac{M_{D^*}}{kp}\left(E-\frac{k^2}{2\mu_*}-\frac{p^2}{2\mu}\right)-i\varepsilon\right) .
\end{aligned}
\tag{2.27}
$$

Note that the projections onto isospin 1/2 are the same as that in the previous subsection, that is, $C_1^I = C_2^I = C_3^I = C_0^I = 1$, and the additional spin projector for the $T_{cc}^* D$ scattering is given by

$$
\mathcal{O}_{j,i}^{J=1}(1\otimes 0\to 1) = \delta_{ij} \, . \tag{2.28}
$$

Using the same strategy as presented in the $T_{cc}^* D^*$ subsection, one can obtain the projection coefficients for the S-wave $T_{cc}^* D$-$T_{cc} D^*$ coupled-channel integral equations by applying the above operators to eqs. (2.25) and (2.26). The results are collected in table 2.

JHEP07(2025)081

Channel	$(I,J)=(1/2,0)$	$(I,J)=(1/2,2)$
$C_4^I C_4^J$	1×1	1×1

Table 3. Coefficients of the partial-wave projected integral equation for the S-wave $T_{cc}D^*$ scattering.

The coupled-channel integral equations are then expressed in the following general form with these spin-isospin factors as,

$$\begin{aligned}(T_1)^{I,J}_{(0)}(E,k,p) &= \int_0^\Lambda dq\, C_1^I C_1^J \mathcal{M}_{12}(p,q)(T_2)^{I,J}_{(0)}(E,k,q)\,,\\ (T_2)^{I,J}_{(0)}(E,k,p) &= C_2^I C_2^J\, \mathcal{M}_{20}(k,p) + \int_0^\Lambda dq\, C_2^I C_2^J \mathcal{M}_{21}(p,q)(T_1)^{I,J}_{(0)}(E,k,q)\\ &\quad + \int_0^\Lambda dq\, C_3^I C_3^J \mathcal{M}_{22}(p,q)(T_2)^{I,J}_{(0)}(E,k,q)\,. \end{aligned} \tag{2.29}$$

The four scalar amplitudes $\mathcal{M}_{12}$, $\mathcal{M}_{20}$, $\mathcal{M}_{21}$, and $\mathcal{M}_{22}$ have been defined by eqs. (2.25) and (2.26). The cutoff dependence of the determinant is shown in figure 7, and again no Efimov effect is observed. The behavior of the phase shifts and scattering lengths is similar to $D^*T_{cc}^*$ system in the previous section, and therefore will not be plotted here and below.

2.5 $T_{cc}D^*$ scattering

Finally, the amplitude for the $J=0$ or $J=2$ S-wave $T_{cc}D^*$ scattering satisfies the single-channel integral equation, as described above, which is given by

$$\begin{aligned}{}_{(0)}T^{lk\beta}_{ji\alpha}(E,k,p) =& -\frac{\pi\gamma_c}{\mu_c^2}\frac{2S_{3,3}}{S_{2,c}c_c}V_3^S(k,p)\,\boxed{\delta_{il}\delta_{kj}\delta_{\beta\alpha}}\\ &-\frac{1}{\pi\mu_c}\frac{S_{3,3}}{S_{2,c}c_c}\int_0^\Lambda dq \frac{q^2\, V_3^S(q,p)\,{}_{(0)}T^{sn\mu}_{ji\alpha}(E,k,q)\,\boxed{\delta_{nl}\delta_{ks}\delta_{\beta\mu}}}{-\gamma_c+\sqrt{-2\mu_c\left(E-\frac{q^2}{2M_{D^*}}-\frac{q^2}{2M_c}\right)-i\varepsilon}}\\ \equiv& \mathcal{M}_0\,\boxed{C_4{}^{lk\beta}_{ji\alpha}} + \int_0^\Lambda dq\,\mathcal{M}_1\,{}_{(0)}T^{sn\mu}_{ji\alpha}(E,k,q)\,\boxed{C_4{}^{lk\beta}_{sn\mu}}. \end{aligned} \tag{2.30}$$

After applying the partial wave projections, one obtains the prefactors as listed in table 3.

Then the projected integral equation for the S-wave $T_{cc}D^*$ scattering reads

$$T^{I,J}_{(0)}(E,k,p) = C_4^I C_4^J\, \mathcal{M}_0(k,p) + \int_0^\Lambda dq\, C_4^I C_4^J \mathcal{M}_1(p,q) T^{I,J}_{(0)}(E,k,q)\,, \tag{2.31}$$

with two scalar amplitudes $\mathcal{M}_0$ and $\mathcal{M}_1$ defined by eq. (2.30). Once again, there is no signal of the Efimov effect in these channels, see figure 8.

3 S-wave $D^*D^*D^*$ system with dimers of all possible quantum numbers

In the preceding section, our analysis demonstrated that the Efimov effect in the coupled-channel Lippmann-Schwinger equation for three-charmed systems involving the T_{cc}^* and T_{cc} dimers is significantly affected by spin, isospin, and symmetry factors arising from identical

JHEP07(2025)081

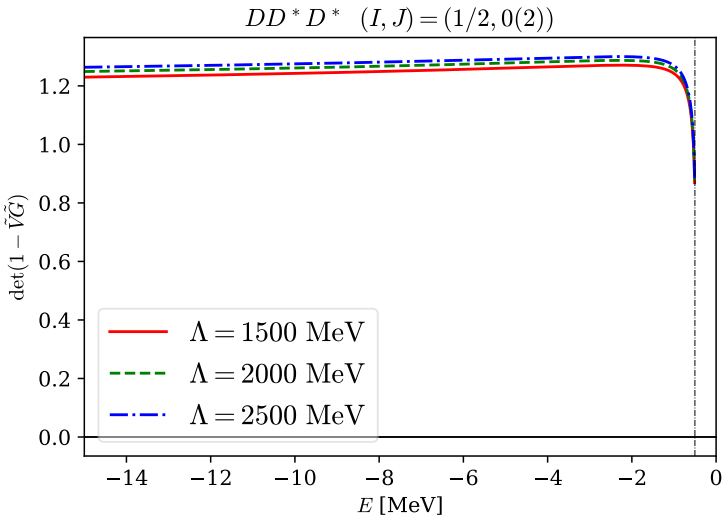

Figure 8. Determinant $\det(1-\tilde{V}\tilde{G})$ of the $T_{cc}D^*$ single-channel scattering equations with quantum numbers $(I,J)=(1/2,0(2))$. The vertical line denotes the threshold of $T_{cc}D^*$.

particles. The weak cutoff dependence in the solutions of the scattering equations shows that there is no Efimov effect when only the $(I,J)=(0,1)$ dimers T_{cc} and T_{cc}^* are present. We will extend our analysis in this section to consider all possible dimer configurations and their implications for Efimov physics. We will focus on the $D^*D^*D^*$ three-body system studied in ref. [78] to investigate under what conditions the Efimov effect can occur.

The Efimov effect emerges from the delicate interplay between short-range two-body interactions and long-range three-body correlations. It depends on the behavior at large momenta within the scattering equation, as exemplified by the three-body scattering equation for identical scalar isoscalar bosons [86, 94]. When the momentum p is much larger than the inverse of the two-body scattering length, the scattering amplitude $T(p)$ satisfies

$$T(p) = \frac{4}{\sqrt{3}\pi p}\int_0^\infty dq\, T(q) \ln\frac{p^2+pq+q^2}{p^2-pq+q^2}. \tag{3.1}$$

By introducing the power-law ansatz $T(p)\sim p^{s-1}$, one obtains in the asymptotic momentum limit,

$$p^s = \frac{4}{\sqrt{3}\pi}\int_0^\infty dq\, q^{s-1} \ln\frac{p^2+pq+q^2}{p^2-pq+q^2}. \tag{3.2}$$

Consequently, a transcendental equation for the scaling parameter s is obtained,

$$1 = \frac{8}{\sqrt{3}}\frac{1}{s}\frac{\sin\frac{\pi}{6}s}{\cos\frac{\pi}{2}s} \tag{3.3}$$

This equation has imaginary solutions $s_0=\pm 1.00624i$, indicating an oscillatory asymptotic behavior for $T(p)$. It becomes necessary to introduce a logarithmic periodic three-body contact interaction to achieve a unique solution as $\Lambda\to\infty$ [86, 94].

This oscillatory behavior manifests as the Efimov effect, characterized by an infinite geometric spectrum of three-body bound states. When two particles interact with a resonant

JHEP07(2025)081

two-body interaction (infinite scattering length), a third particle can induce an effective attractive interaction, leading to the formation of weakly bound three-body states. These Efimov states follow a geometric scaling pattern, with each consecutive energy level related by a universal scaling factor of approximately $e^{2\pi/|s_0|} \approx 515$, as given in eq. (1.1). This remarkable phenomenon is universal, appearing in nuclear physics, atomic physics, and other quantum systems regardless of the underlying short-range interactions (for a review, see ref. [59]).

When the bosons have spin and isospin, there will be various channels with different CG coefficients and symmetry factors. Then the asymptotic behavior of scattering equation will depend on these CG coefficients and symmetry factors. For coupled-channel scattering equations, if all scattering lengths are unnaturally large, eq. (3.1) is generalized to

$$T_i(p) = \mathcal{A}_{ij} \frac{4}{\sqrt{3}\pi p} \int_0^\infty dq\, T_j(q) \frac{1}{2} \ln \frac{p^2 + pq + q^2}{p^2 - pq + q^2}. \tag{3.4}$$

The factor $\mathcal{A}_{ij}$ contributes to the coefficient of the scattering equations. One can decouple the above coupled-channel scattering equation into single-channel equations of $\hat{T}_i(p)$ by a unitary transformation $\mathcal{S}$, which diagonalizes $\mathcal{A}$ to $\mathcal{S}^{-1}\mathcal{A}\mathcal{S} = \mathrm{diag}(\lambda_1, \lambda_2, \ldots)$, as (cf. ref. [96])

$$\begin{pmatrix} T_1 \\ T_2 \\ \ldots \end{pmatrix} = \mathcal{S} \begin{pmatrix} \hat{T}_1 \\ \hat{T}_2 \\ \ldots \end{pmatrix}. \tag{3.5}$$

The behavior of each $\hat{T}_i(p)$ is governed by the corresponding eigenvalue λ_i of $\mathcal{A}$. Using the ansatz $\hat{T}_i(p) \sim p^{s_i - 1}$, we obtain equations for s_i:

$$1 = \frac{4\lambda_i}{\sqrt{3}} \frac{1}{s_i} \frac{\sin \frac{\pi}{6} s_i}{\cos \frac{\pi}{2} s_i} \tag{3.6}$$

The Efimov effect occurs in the system when this equation has an imaginary solution, which happens when $\lambda_i > \lambda_c = 3\sqrt{3}/(2\pi) \approx 0.826993$ [59]. It is worth noting that for a system of three identical scalar bosons without (iso)spin, $\lambda = 2$ as shown in eq. (3.3).

It should be noted that the Bose-Einstein statistics plays a significant role in this context. The matrix $\mathcal{A}$ contains the symmetry factor S_3 from the one-boson exchange diagram, as defined in eq. (2.8), as well as the spin and isospin CG coefficients, the two-body symmetry factor S_2, and the normalization constant c in G_A. We summarize the matrix $\mathcal{A}$ and its eigenvalues λ_i for the $D^*D^*D^*$ system in table 4.

Therefore, for the $D^*D^*D^*$ system, we conclude in section 2 that no Efimov effect occurs when only the existence of the T_{cc}^* dimer with quantum numbers $(I, J) = (0, 1)$ is assumed. However, when dimers with quantum numbers $(I, J) = (1, 2)$ and $(1, 0)$ are included in eq. (3.4) (that is, these two-body D^*D^* channels approach the unitary limit), the Efimov effect emerges in channels where the eigenvalue equals 2, exceeding the critical threshold λ_c. In these cases, the scaling factor s_i for the Efimov states equals $\pm 1.00624i$, which precisely matches the value observed in systems of three identical spinless and isoscalar bosons. In particular, for the $(I, J) = (1/2, 2)$ system, the Efimov effect can emerge if, in addition to the existence of the isoscalar T_{cc}^*, the D^*D^* scattering length in the $(I, J) = (1, 2)$ channel is sufficiently large.

Let us take the case of $(I, J) = (1/2, 1)$ in table 4 as an example. If we set all three D^*D^* dimers $(1, 0)$, $(0, 1)$, and $(1, 2)$ with binding energies equal to 0.50 MeV (corresponding

JHEP07(2025)081

(I,J)	$\mathcal{A}$	λ_i
$(1/2,0)$	-1	-1
$(3/2,0)$	-	-
$(1/2,1)$	$\begin{pmatrix} -\frac{1}{3} & 1 & -\frac{\sqrt{5}}{3} \\ 1 & \frac{1}{2} & -\frac{\sqrt{5}}{2} \\ -\frac{\sqrt{5}}{3} & -\frac{\sqrt{5}}{2} & -\frac{1}{6} \end{pmatrix}$	$2,-1,-1$
$(3/2,1)$	$\begin{pmatrix} \frac{2}{3} & \frac{2\sqrt{5}}{3} \\ \frac{2\sqrt{5}}{3} & \frac{1}{3} \end{pmatrix}$	$2,-1$
$(1/2,2)$	$\begin{pmatrix} \frac{1}{2} & \frac{3}{2} \\ \frac{3}{2} & \frac{1}{2} \end{pmatrix}$	$2,-1$
$(3/2,2)$	-1	-1
$(1/2,3)$	-1	-1
$(3/2,3)$	2	2

Table 4. The $\mathcal{A}$ matrix and its eigenvalues λ_i for the $D^*D^*D^*$ three-body scattering equation with various (I,J) quantum numbers. The row and column indices of $\mathcal{A}_{ij}$ represent the three possible dimers with quantum numbers $(I,J)=(1,0)$, $(0,1)$, and $(1,2)$, respectively, when they contribute to the channel. Specifically, for $(I,J)=(1/2,1)$, all three dimers contribute to the coupled-channel system, so index 1 corresponds to $(1,0)$, index 2 to $(0,1)$, and index 3 to $(1,2)$. For $(I,J)=(3/2,1)$, only dimers with $(I,J)=(1,0)$ and $(1,2)$ contribute, so we use index 1 for $(1,0)$ and index 2 for $(1,2)$. For $(I,J)=(1/2,2)$, only dimers with $(I,J)=(0,1)$ and $(1,2)$ contribute, so we use index 1 for $(0,1)$ and index 2 for $(1,2)$. The case of $(I,J)=(3/2,0)$ is forbidden by the Bose-Einstein statistics.

to the binding energy of T_{cc}^*), when $\Lambda = 1500\,\text{MeV}$ we can find the first two bound states located at $E_1 = -44.3\,\text{MeV}$ and $E_2 = -0.83\,\text{MeV}$ with a vanishing three-body force. It is noteworthy that $\Delta E_1/\Delta E_2 \approx 134$ with $\Delta E_n = E_n + E_B^*$, which is similar to the result with the same value of binding energy in ref. [78].

4 Summary and discussions

The existence of the $T_{cc}(3875)^+$ extremely close to the DD^* threshold implies a large S-wave scattering length in the isoscalar DD^* channel. Motivated by this observation and the hypothetical heavy quark spin partner of the T_{cc}, denoted as T_{cc}^* with quantum numbers $(I,J)=(0,1)$, we have investigated the possibility of the Efimov effect in the $D^*D^*D^*$ and DD^*D^* three-body systems. Our analysis reveals that if only the isoscalar $J=1$ dimers T_{cc} and T_{cc}^* exist, no Efimov effect is expected. This conclusion differs from that of ref. [78], which reported the existence of $(I,J)=(1/2,0)$ $D^*D^*D^*$ three-body bound states due to the inconsistent prefactors arising from the partial wave projection.

Then we investigate under what conditions there can be Efimov effects in the S-wave $D^*D^*D^*$ system. We find that if the unitary limit is approached also in the isovector $(I,J)=(1,0)$ and $(I,J)=(1,2)$ D^*D^* channels, the Efimov effect can be reinstated. Notice that such a case corresponds to one of the solutions of minimizing the entanglement [97]

JHEP07(2025)081

for the S-wave $D^{(*)}D^{(*)}$ scatterings [98]. However, since the partial decay width of the $T_{cc}^* \to DD^*$ channel could reach around 20 MeV [85], Efimov states in $D^*D^*D^*$ — if they exist at all by satisfying the conditions mentioned above — will be hard to be found in experiments. It would be interesting to calculate the isovector D^*D^* low-energy scatterings with $J = 1$ and 2 using lattice QCD.

Acknowledgments

This work is supported in part by the National Key R&D Program of China under Grant No. 2023YFA1606703; by the National Natural Science Foundation of China (NSFC) under Grants No. 12125507, No. 12361141819, and No. 12447101; by the Chinese Academy of Sciences (CAS) under Grant No. YSBR-101. U.-G.M. and A.R. are also partially supported by the CAS President's International Fellowship Initiative (PIFI) under Grant Nos. 2025PD0022 and 2024VMB0001, respectively. The work of UGM was also supported by the European Research Council (ERC) under the European Union's Horizon 2020 research and innovation programme (grant agreement No. 101018170). And AR in addition acknowledges the financial support from the Ministry of Culture and Science of North Rhine-Westphalia through the NRW-FAIR program. H.-L.F. thanks the University of Bonn and Y.-H.L. thanks the Institute of Theoretical Physics, CAS, for the hospitality during their visits. H.-W.H. was supported by Deutsche Forschungsgemeinschaft (DFG, German Research Foundation) under Project ID 279384907 — SFB 1245 and by the German Federal Ministry of Education and Research (BMBF) (Grant No. 05P24RDB).

Data Availability Statement. This article has no associated data or the data will not be deposited.

Code Availability Statement. This article has no associated code or the code will not be deposited.

References

[1] M.Y. Barabanov et al., *Diquark correlations in hadron physics: Origin, impact and evidence*, *Prog. Part. Nucl. Phys.* **116** (2021) 103835 [arXiv:2008.07630] [INSPIRE].

[2] H.-X. Chen et al., *An updated review of the new hadron states*, *Rept. Prog. Phys.* **86** (2023) 026201 [arXiv:2204.02649] [INSPIRE].

[3] N. Brambilla et al., *The XYZ states: experimental and theoretical status and perspectives*, *Phys. Rept.* **873** (2020) 1 [arXiv:1907.07583] [INSPIRE].

[4] X.-K. Dong, F.-K. Guo and B.-S. Zou, *A survey of heavy–heavy hadronic molecules*, *Commun. Theor. Phys.* **73** (2021) 125201 [arXiv:2108.02673] [INSPIRE].

[5] A. Esposito, A. Pilloni and A.D. Polosa, *Multiquark Resonances*, *Phys. Rept.* **668** (2017) 1 [arXiv:1611.07920] [INSPIRE].

JHEP07(2025)081

[6] F.-K. Guo et al., *Hadronic molecules*, *Rev. Mod. Phys.* **90** (2018) 015004 [*Erratum ibid.* **94** (2022) 029901] [arXiv:1705.00141] [INSPIRE].

[7] F.-K. Guo, X.-H. Liu and S. Sakai, *Threshold cusps and triangle singularities in hadronic reactions*, *Prog. Part. Nucl. Phys.* **112** (2020) 103757 [arXiv:1912.07030] [INSPIRE].

[8] A. Hosaka et al., *Exotic hadrons with heavy flavors: X, Y, Z, and related states*, *PTEP* **2016** (2016) 062C01 [arXiv:1603.09229] [INSPIRE].

[9] R.F. Lebed, R.E. Mitchell and E.S. Swanson, *Heavy-Quark QCD Exotica*, *Prog. Part. Nucl. Phys.* **93** (2017) 143 [arXiv:1610.04528] [INSPIRE].

[10] Y.-R. Liu et al., *Pentaquark and Tetraquark states*, *Prog. Part. Nucl. Phys.* **107** (2019) 237 [arXiv:1903.11976] [INSPIRE].

[11] M. Mai, U.-G. Meißner and C. Urbach, *Towards a theory of hadron resonances*, *Phys. Rept.* **1001** (2023) 1 [arXiv:2206.01477] [INSPIRE].

[12] S.L. Olsen, T. Skwarnicki and D. Zieminska, *Nonstandard heavy mesons and baryons: Experimental evidence*, *Rev. Mod. Phys.* **90** (2018) 015003 [arXiv:1708.04012] [INSPIRE].

[13] G. Yang, J. Ping and J. Segovia, *Tetra- and penta-quark structures in the constituent quark model*, *Symmetry* **12** (2020) 1869 [arXiv:2009.00238] [INSPIRE].

[14] J.-H. Chen et al., *Production of exotic hadrons in pp and nuclear collisions*, *Nucl. Sci. Tech.* **36** (2025) 55 [arXiv:2411.18257] [INSPIRE].

[15] M.-Z. Liu et al., *Three ways to decipher the nature of exotic hadrons: Multiplets, three-body hadronic molecules, and correlation functions*, *Phys. Rept.* **1108** (2025) 1 [arXiv:2404.06399] [INSPIRE].

[16] Z.-G. Wang, *Review of the QCD sum rules for exotic states*, arXiv:2502.11351 [INSPIRE].

[17] L. Castillejo, R.H. Dalitz and F.J. Dyson, *Low's scattering equation for the charged and neutral scalar theories*, *Phys. Rev.* **101** (1956) 453 [INSPIRE].

[18] X.-W. Kang and J.A. Oller, *Different pole structures in line shapes of the $X(3872)$*, *Eur. Phys. J. C* **77** (2017) 399 [arXiv:1612.08420] [INSPIRE].

[19] L.R. Dai, J. Song and E. Oset, *Evolution of genuine states to molecular ones: The Tcc(3875) case*, *Phys. Lett. B* **846** (2023) 138200 [arXiv:2306.01607] [INSPIRE].

[20] J. Song, L.R. Dai and E. Oset, *Evolution of compact states to molecular ones with coupled channels: The case of the X(3872)*, *Phys. Rev. D* **108** (2023) 114017 [arXiv:2307.02382] [INSPIRE].

[21] V. Baru et al., *Effective range expansion for narrow near-threshold resonances*, *Phys. Lett. B* **833** (2022) 137290 [arXiv:2110.07484] [INSPIRE].

[22] R. Blankenbecler and R. Sugar, *Linear integral equations for relativistic multichannel scattering*, *Phys. Rev.* **142** (1966) 1051 [INSPIRE].

[23] R. Aaron, R.D. Amado and J.E. Young, *Relativistic three-body theory with applications to pi-minus n scattering*, *Phys. Rev.* **174** (1968) 2022 [INSPIRE].

[24] R. Blankenbecler, *Construction of Unitary Scattering Amplitudes*, *Phys. Rev.* **122** (1961) 983 [INSPIRE].

[25] L.F. Cook and B.W. Lee, *Unitarity and Production Amplitudes*, *Phys. Rev.* **127** (1962) 283 [INSPIRE].

JHEP07(2025)081

[26] G.N. Fleming, *Recoupling Effects in the Isobar Model. 1. General Formalism for Three-Pion Scattering*, *Phys. Rev.* **135** (1964) B551 [INSPIRE].

[27] M.T. Grisaru, *Three-Particle Contributions to Elastic Scattering*, *Phys. Rev.* **146** (1966) 1098 [INSPIRE].

[28] R. Aaron and R.D. Amado, *Analysis of three-hadron final states*, *Phys. Rev. Lett.* **31** (1973) 1157 [INSPIRE].

[29] R.D. Amado, *Minimal three-body scattering theory*, *Phys. Rev. Lett.* **33** (1974) 333 [INSPIRE].

[30] M. Mai et al., *Three-body Unitarity with Isobars Revisited*, *Eur. Phys. J. A* **53** (2017) 177 [arXiv:1706.06118] [INSPIRE].

[31] M. Mai and M. Döring, *Three-body Unitarity in the Finite Volume*, *Eur. Phys. J. A* **53** (2017) 240 [arXiv:1709.08222] [INSPIRE].

[32] H.-W. Hammer, J.-Y. Pang and A. Rusetsky, *Three-particle quantization condition in a finite volume: 1. The role of the three-particle force*, *JHEP* **09** (2017) 109 [arXiv:1706.07700] [INSPIRE].

[33] H.-W. Hammer, J.-Y. Pang and A. Rusetsky, *Three particle quantization condition in a finite volume: 2. general formalism and the analysis of data*, *JHEP* **10** (2017) 115 [arXiv:1707.02176] [INSPIRE].

[34] M. Döring et al., *Three-body spectrum in a finite volume: the role of cubic symmetry*, *Phys. Rev. D* **97** (2018) 114508 [arXiv:1802.03362] [INSPIRE].

[35] JPAC collaboration, *Phenomenology of Relativistic* $\mathbf{3} \to \mathbf{3}$ *Reaction Amplitudes within the Isobar Approximation*, *Eur. Phys. J. C* **79** (2019) 56 [arXiv:1809.10523] [INSPIRE].

[36] S.M. Dawid and A.P. Szczepaniak, *Bound states in the B-matrix formalism for the three-body scattering*, *Phys. Rev. D* **103** (2021) 014009 [arXiv:2010.08084] [INSPIRE].

[37] F. Müller, J.-Y. Pang, A. Rusetsky and J.-J. Wu, *Relativistic-invariant formulation of the NREFT three-particle quantization condition*, *JHEP* **02** (2022) 158 [arXiv:2110.09351] [INSPIRE].

[38] M.T. Hansen and S.R. Sharpe, *Relativistic, model-independent, three-particle quantization condition*, *Phys. Rev. D* **90** (2014) 116003 [arXiv:1408.5933] [INSPIRE].

[39] M.T. Hansen and S.R. Sharpe, *Expressing the three-particle finite-volume spectrum in terms of the three-to-three scattering amplitude*, *Phys. Rev. D* **92** (2015) 114509 [arXiv:1504.04248] [INSPIRE].

[40] T.D. Blanton and S.R. Sharpe, *Alternative derivation of the relativistic three-particle quantization condition*, *Phys. Rev. D* **102** (2020) 054520 [arXiv:2007.16188] [INSPIRE].

[41] R.A. Briceño, M.T. Hansen and S.R. Sharpe, *Relating the finite-volume spectrum and the two-and-three-particle S matrix for relativistic systems of identical scalar particles*, *Phys. Rev. D* **95** (2017) 074510 [arXiv:1701.07465] [INSPIRE].

[42] R.A. Briceño, M.T. Hansen and S.R. Sharpe, *Three-particle systems with resonant subprocesses in a finite volume*, *Phys. Rev. D* **99** (2019) 014516 [arXiv:1810.01429] [INSPIRE].

[43] M.T. Hansen, F. Romero-López and S.R. Sharpe, *Generalizing the relativistic quantization condition to include all three-pion isospin channels*, *JHEP* **07** (2020) 047 [*Erratum ibid.* **02** (2021) 014] [arXiv:2003.10974] [INSPIRE].

[44] T.D. Blanton and S.R. Sharpe, *Equivalence of relativistic three-particle quantization conditions*, *Phys. Rev. D* **102** (2020) 054515 [arXiv:2007.16190] [INSPIRE].

JHEP07(2025)081

[45] T.D. Blanton and S.R. Sharpe, *Three-particle finite-volume formalism for $\pi^+\pi^+K^+$ and related systems*, *Phys. Rev. D* **104** (2021) 034509 [arXiv:2105.12094] [INSPIRE].

[46] U.-G. Meißner, G. Ríos and A. Rusetsky, *Spectrum of three-body bound states in a finite volume*, *Phys. Rev. Lett.* **114** (2015) 091602 [*Erratum ibid.* **117** (2016) 069902] [arXiv:1412.4969] [INSPIRE].

[47] B. Hörz and A. Hanlon, *Two- and three-pion finite-volume spectra at maximal isospin from lattice QCD*, *Phys. Rev. Lett.* **123** (2019) 142002 [arXiv:1905.04277] [INSPIRE].

[48] T.D. Blanton, F. Romero-López and S.R. Sharpe, *$I = 3$ Three-Pion Scattering Amplitude from Lattice QCD*, *Phys. Rev. Lett.* **124** (2020) 032001 [arXiv:1909.02973] [INSPIRE].

[49] M. Mai, M. Döring, C. Culver and A. Alexandru, *Three-body unitarity versus finite-volume $\pi^+\pi^+\pi^+$ spectrum from lattice QCD*, *Phys. Rev. D* **101** (2020) 054510 [arXiv:1909.05749] [INSPIRE].

[50] C. Culver et al., *Three pion spectrum in the $I = 3$ channel from lattice QCD*, *Phys. Rev. D* **101** (2020) 114507 [arXiv:1911.09047] [INSPIRE].

[51] M. Fischer et al., *Scattering of two and three physical pions at maximal isospin from lattice QCD*, *Eur. Phys. J. C* **81** (2021) 436 [arXiv:2008.03035] [INSPIRE].

[52] R. Brett et al., *Three-body interactions from the finite-volume QCD spectrum*, *Phys. Rev. D* **104** (2021) 014501 [arXiv:2101.06144] [INSPIRE].

[53] T.D. Blanton et al., *Interactions of two and three mesons including higher partial waves from lattice QCD*, *JHEP* **10** (2021) 023 [arXiv:2106.05590] [INSPIRE].

[54] A. Alexandru et al., *Finite-volume energy spectrum of the $K^-K^-K^-$ system*, *Phys. Rev. D* **102** (2020) 114523 [arXiv:2009.12358] [INSPIRE].

[55] Z.T. Draper et al., *Interactions of πK, $\pi\pi K$ and $KK\pi$ systems at maximal isospin from lattice QCD*, *JHEP* **05** (2023) 137 [arXiv:2302.13587] [INSPIRE].

[56] HADRON SPECTRUM collaboration, *Energy-Dependent $\pi^+\pi^+\pi^+$ Scattering Amplitude from QCD*, *Phys. Rev. Lett.* **126** (2021) 012001 [arXiv:2009.04931] [INSPIRE].

[57] V. Efimov, *Energy levels arising form the resonant two-body forces in a three-body system*, *Phys. Lett. B* **33** (1970) 563 [INSPIRE].

[58] C. Chin, R. Grimm, P. Julienne and E. Tiesinga, *Feshbach resonances in ultracold gases*, *Rev. Mod. Phys.* **82** (2010) 1225 [INSPIRE].

[59] E. Braaten and H.-W. Hammer, *Universality in few-body systems with large scattering length*, *Phys. Rept.* **428** (2006) 259 [cond-mat/0410417] [INSPIRE].

[60] V.N. Efimov, *Weakly-bound states of 3 resonantly-interacting particles*, *Sov. J. Nucl. Phys.* **12** (1971) 589 [INSPIRE].

[61] E. Braaten, H.W. Hammer and M. Kusunoki, *Universal equation for Efimov states*, *Phys. Rev. A* **67** (2003) 022505 [cond-mat/0201281] [INSPIRE].

[62] T. Kraemer et al., *Evidence for Efimov quantum states in an ultracold gas of caesium atoms*, *Nature* **440** (2006) 315.

[63] P. Naidon and S. Endo, *Efimov Physics: a review*, *Rept. Prog. Phys.* **80** (2017) 056001 [arXiv:1610.09805] [INSPIRE].

[64] H.-W. Hammer and L. Platter, *Efimov States in Nuclear and Particle Physics*, *Ann. Rev. Nucl. Part. Sci.* **60** (2010) 207 [arXiv:1001.1981] [INSPIRE].

JHEP07(2025)081

[65] E. Epelbaum, H.-W. Hammer and U.-G. Meissner, *Modern Theory of Nuclear Forces*, *Rev. Mod. Phys.* **81** (2009) 1773 [arXiv:0811.1338] [INSPIRE].

[66] H.-W. Hammer, C. Ji and D.R. Phillips, *Effective field theory description of halo nuclei*, *J. Phys. G* **44** (2017) 103002 [arXiv:1702.08605] [INSPIRE].

[67] H.-W. Hammer, S. König and U. van Kolck, *Nuclear effective field theory: status and perspectives*, *Rev. Mod. Phys.* **92** (2020) 025004 [arXiv:1906.12122] [INSPIRE].

[68] BELLE collaboration, *Observation of a narrow charmonium-like state in exclusive $B^{\pm} \to K^{\pm}\pi^{+}\pi^{-}J/\psi$ decays*, *Phys. Rev. Lett.* **91** (2003) 262001 [hep-ex/0309032] [INSPIRE].

[69] LHCB collaboration, *Study of the doubly charmed tetraquark T_{cc}^{+}*, *Nature Commun.* **13** (2022) 3351 [arXiv:2109.01056] [INSPIRE].

[70] E. Braaten and M. Kusunoki, *Low-energy universality and the new charmonium resonance at 3870-MeV*, *Phys. Rev. D* **69** (2004) 074005 [hep-ph/0311147] [INSPIRE].

[71] D.L. Canham, H.-W. Hammer and R.P. Springer, *On the scattering of D and D* mesons off the X(3872)*, *Phys. Rev. D* **80** (2009) 014009 [arXiv:0906.1263] [INSPIRE].

[72] M.P. Valderrama, *$\bar{D}^{*}\bar{D}^{*}\Sigma_c$ three-body system*, *Phys. Rev. D* **99** (2019) 034010 [arXiv:1811.10173] [INSPIRE].

[73] A. Martinez Torres, K.P. Khemchandani, L. Roca and E. Oset, *Few-body systems consisting of mesons*, *Few Body Syst.* **61** (2020) 35 [arXiv:2005.14357] [INSPIRE].

[74] M.P. Valderrama, *$D^{*}D^{*}\bar{D}$ and $D^{*}D^{*}\bar{D}^{*}$ three-body systems*, *Phys. Rev. D* **98** (2018) 034017 [arXiv:1805.10584] [INSPIRE].

[75] Z.-G. Wang, *Analysis of the tetraquark and hexaquark molecular states with the QCD sum rules*, *Commun. Theor. Phys.* **73** (2021) 065201 [arXiv:2003.10631] [INSPIRE].

[76] S.-Q. Luo et al., *Triple-charm molecular states composed of D*D*D and D*D*D*, *Phys. Rev. D* **105** (2022) 074033 [arXiv:2111.15079] [INSPIRE].

[77] M. Bayar et al., *Exotic states with triple charm*, *Eur. Phys. J. C* **83** (2023) 46 [arXiv:2211.09294] [INSPIRE].

[78] P.G. Ortega, *Exploring the Efimov effect in the D*D*D* system*, *Phys. Rev. D* **110** (2024) 034015 [arXiv:2403.10244] [INSPIRE].

[79] H.-X. Zhu et al., *Constraining the DDD* three-body bound state via the Zc(3900) pole*, *Phys. Rev. D* **111** (2025) 094022 [arXiv:2412.12816] [INSPIRE].

[80] M. Albaladejo, *Tcc+ coupled channel analysis and predictions*, *Phys. Lett. B* **829** (2022) 137052 [arXiv:2110.02944] [INSPIRE].

[81] M.-L. Du et al., *Coupled-channel approach to Tcc+ including three-body effects*, *Phys. Rev. D* **105** (2022) 014024 [arXiv:2110.13765] [INSPIRE].

[82] Z.-S. Jia et al., *Hadronic decays of the heavy-quark-spin molecular partner of Tcc+*, *Phys. Rev. D* **107** (2023) 074029 [arXiv:2211.02479] [INSPIRE].

[83] Z.-S. Jia, Z.-H. Zhang, G. Li and F.-K. Guo, *Radiative decays of the heavy-quark-spin molecular partner of Tcc+*, *Phys. Rev. D* **108** (2023) 094038 [arXiv:2307.11047] [INSPIRE].

[84] R. Molina, T. Branz and E. Oset, *A new interpretation for the $D_{s2}^{*}(2573)$ and the prediction of novel exotic charmed mesons*, *Phys. Rev. D* **82** (2010) 014010 [arXiv:1005.0335] [INSPIRE].

JHEP07(2025)081

[85] L.R. Dai, R. Molina and E. Oset, *Prediction of new Tcc states of D*D* and Ds*D* molecular nature*, *Phys. Rev. D* **105** (2022) 016029 [*Erratum ibid.* **106** (2022) 099902] [arXiv:2110.15270] [INSPIRE].

[86] P.F. Bedaque, H.W. Hammer and U. van Kolck, *Renormalization of the three-body system with short range interactions*, *Phys. Rev. Lett.* **82** (1999) 463 [nucl-th/9809025] [INSPIRE].

[87] E. Wilbring, *Efimov Effect in Pionless Effective Field Theory and its Application to Hadronic Molecules*, Ph.D. thesis, Bonn University, Germany (2016) [INSPIRE].

[88] Y.-H. Lin et al., *Three-body universality in the B meson sector*, arXiv:1705.06176 [INSPIRE].

[89] LHCB collaboration, *Observation of an exotic narrow doubly charmed tetraquark*, *Nature Phys.* **18** (2022) 751 [arXiv:2109.01038] [INSPIRE].

[90] L. Meng et al., *Doubly charm tetraquark channel with isospin 1 from lattice QCD*, *Phys. Rev. D* **111** (2025) 034509 [arXiv:2411.06266] [INSPIRE].

[91] P.-P. Shi et al., *Low-energy DD scattering in lattice QCD*, arXiv:2502.07438 [INSPIRE].

[92] D.B. Kaplan, M.J. Savage and M.B. Wise, *Two nucleon systems from effective field theory*, *Nucl. Phys. B* **534** (1998) 329 [nucl-th/9802075] [INSPIRE].

[93] D.B. Kaplan, M.J. Savage and M.B. Wise, *A new expansion for nucleon-nucleon interactions*, *Phys. Lett. B* **424** (1998) 390 [nucl-th/9801034] [INSPIRE].

[94] P.F. Bedaque, H.W. Hammer and U. van Kolck, *The three boson system with short range interactions*, *Nucl. Phys. A* **646** (1999) 444 [nucl-th/9811046] [INSPIRE].

[95] D.B. Kaplan, J.-W. Lee, D.T. Son and M.A. Stephanov, *Conformality Lost*, *Phys. Rev. D* **80** (2009) 125005 [arXiv:0905.4752] [INSPIRE].

[96] F. Hildenbrand and H.-W. Hammer, *Three-Body Hypernuclei in Pionless Effective Field Theory*, *Phys. Rev. C* **100** (2019) 034002 [*Erratum ibid.* **102** (2020) 039901] [arXiv:1904.05818] [INSPIRE].

[97] S.R. Beane, D.B. Kaplan, N. Klco and M.J. Savage, *Entanglement Suppression and Emergent Symmetries of Strong Interactions*, *Phys. Rev. Lett.* **122** (2019) 102001 [arXiv:1812.03138] [INSPIRE].

[98] T.-R. Hu, S. Chen and F.-K. Guo, *Entanglement suppression and low-energy scattering of heavy mesons*, *Phys. Rev. D* **110** (2024) 014001 [arXiv:2404.05958] [INSPIRE].

JHEP07(2025)081